Epitope Insertion Favors a Six Transmembrane Domain Model for the Carboxy-Terminal Portion of the Multidrug Resistance-Associated Protein†

Christina Kast and Philippe Gros*

Department of Biochemistry, McGill University, 3655 Drummond, Montreal, Quebec, Canada H3G 1Y6

Received September 19, 1997; Revised Manuscript Received November 21, 1997

ABSTRACT: The overexpression of the multidrug resistance protein, MRP, in mammalian cells is associated with pleiotropic resistance to cytotoxic drugs. MRP is an integral membrane protein which belongs to the family of ATP-binding cassette transporters. Secondary structure predictions combined with biochemical analyses suggest that MRP encodes 11 transmembrane (TM) domains in the amino-terminal half of the protein and four or six transmembrane domains in the carboxy-terminal half of the protein. To gain insight into the membrane topology of the carboxy-terminal half of MRP, small, antigenic hemagglutinin (HA) epitopes (YPYDVPDYAS) were inserted within six predicted hydrophilic subfragments of this region (938, 1001, 1084, 1175, 1222, 1295). These epitope-tagged MRP variants were expressed in HeLa cells to evaluate their ability to confer resistance to the drug etoposide (VP-16). Insertion of the HA epitopes at positions 938, 1001, and 1222 resulted in functional proteins, while epitope insertion at positions 1084, 1175, and 1295 abrogated MRP function. The intracellular versus extracellular location of the HA epitopes present in biologically active MRP variants was then established in intact and permeabilized cells by immunofluorescence using an anti-HA antibody. Epitopes inserted at positions 1001 and 1222 were located on the extracellular side of the plasma membrane, while the epitope inserted at position 938 was located intracellularly. These results are consistent with a six TM rather than a four TM domain model for the membrane portion of the carboxy-terminal half of MRP.

Cellular resistance to structurally unrelated chemotherapeutic agents is a major limitation to the successful treatment of many types of human cancers (*1*). In vivo, multidrug resistance (MDR) is caused by independent overexpression of two families of integral membrane proteins, P-glycoprotein (P-gp) and the multidrug resistance-associated protein (MRP)[1] (*2*, *3*). These proteins have been proposed to act as ATP-dependent membrane pumps with broad substrate specificity (*4*−*7*).

Human *MRP1* was cloned as an mRNA overexpressed in a P-gp negative, Adriamycin-resistant, H69AR small cell lung carcinoma cell line (*8*) and was subsequently shown to confer resistance to cytotoxic drugs such as doxorubicin, *Vinca* alkaloids, and epipodophyllotoxins when overexpressed in transfection experiments (*9*). Studies in inside-out membrane vesicles further suggested that MRP1 could transport glutathione conjugates (*10*), most notably cysteinyl leukotrienes (*11*, *12*), anionic conjugates of bile salts and steroid hormones (*13*), and glutathione conjugates of chemotherapeutic agents (*14*). MRP defines a gene family that contains at least five members designated *MRP1* to *MRP5* (*15*). MRP2 (also known as cMOAT) is closely related to MRP1 and is predominantly expressed on the canalicular membrane of hepatocytes. MRP2 appears responsible for the secretion of amphiphilic anionic conjugates into the bile, and a mutation in the *rMrp2* gene of TR^- mutant rats is associated with a defect in the biliary transport of organic anions (*16*, *17*). Likewise, a non-sense mutation at Arg^{1066} of human *MRP2* has been detected in Dubin−Johnson syndrome, a pathology characterized by a defect in hepatic multispecific organic anion transport (*18*, *19*). The function of the other members of the MRP gene family remains to be fully clarified. *MRP3* and *MRP5* expression is elevated in a series of multidrug- or cisplatin-resistant cell lines; however, expression does not seem to correlate with resistance to doxorubicin or cisplatin. In this study, *MRP4* was not overexpressed in any of the drug-resistant cell lines tested (*15*).

Both MRP and P-gp belong to a larger family known as the ATP-binding cassette (ABC) superfamily of transport proteins (*20*). Within this gene family, MRP forms a structurally and functionally distinct subgroup that includes the yeast cadmium resistance factor YCF1 (43% amino acid sequence identity, *21*), the yeast YORI protein (33% identity) that mediates oligomycin resistance (*22*), the bile acid transporter BAT1 (*23*), the *Leishmania tarentolae* P-gpA

† This work was supported by a research grant to P.G. from the Cancer Research Society. P.G. is supported by a career award from the Medical Research Council of Canada and is an International Research Scholar of the Howard Hughes Medical Institute.

* To whom all correspondence should be addressed. Phone: 514-398-7291. FAX: 514-398-2603. E-mail: gros@medcor.mcgill.ca.

[1] ABC, ATP-binding cassette; ACT, actinomycin-D; ADM, Adriamycin; BAT1, bile acid transporter; BSA, bovine serum albumin; CFTR, cystic fibrosis transmembrane conductance regulator; DMEM, Dulbecco's modified Eagle's medium; EBCR, cyclic AMP activated epithelial basolateral chloride conductance regulator; HA, hemagglutinin; MAR, membrane-associated region; MRP, multidrug resistance-associated protein; NBD, nucleotide-binding domain; P-gp, P-glycoprotein; SDS−PAGE, sodium dodecyl sulfate−polyacrylamide gel electrophoresis; SUR, sulfonylurea receptor; TM, transmembrane; VCR, vincristine; VP-16, etoposide; YCF1, yeast cadmium factor I; YORI, yeast oligomycin resistance I.

S0006-2960(97)02332-5 CCC: $15.00
Published on Web 02/04/1998

(32% identity) associated with resistance to arsenicals and antimony (*24*, *25*), the mammalian sulfonylurea receptors SUR1 and SUR2 (rSUR1: 29% identity) (*26*, *27*), and the cAMP-activated epithelial basolateral chloride conductance regulator EBCR (*28*). Alignment of primary amino acid sequences and hydropathy profiles of several members of this family indicates that, in contrast to P-gp (*29*) and CFTR (*30*), which are formed by two sequence homologous halves each encoding six putative transmembrane (TM) domains and one nucleotide-binding domain (NBD) (*31*−*34*), the MRP group contains an additional, highly hydrophobic, membrane-associated region (MAR) at the amino terminus (*35*−*39*). Studies of glycosylation-site mutants (*37*) and immunofluorescence studies of MRP mutants containing epitope tags (*38*) have shown that the amino terminus of MRP is extracellular. In addition, these studies (*37*, *38*), together with the mapping of an intracellular protease hypersensitive site to the linker region connecting MAR1 and MAR2 (*40*), have suggested an odd number of five TM domains for the N-terminal MAR1 region of MRP. Hydropathy analyses (*35*−*37*) and direct topological data (*38*, *40*, *43*) suggest that MAR2 would include six TM domains, in a structural arrangement similar to that seen in the corresponding region of P-gp and CFTR (*36*, *37*). For the third, carboxy-terminal MAR3 of MRP, alternate topological models of four (*8*, *37*) or six TM domains have been proposed (*36*, *37*) on the basis of hydropathy profiling using different computer programs. Direct experimental topological data of this carboxy-terminal half of MRP includes antibody epitope mapping studies positioning residues 918−924 (QCRL-1 antibody epitope) within the linker sequence connecting NBD1 to the carboxy-terminal half of the protein (L-2) intracellularly (*42*, *43*). In addition, Asn^{1006} was recently shown to be glycosylated and most likely positioned extracellularly, between the first and second TM domains of the MAR3 region (*37*). Finally, an antibody directed against a fusion protein consisting of residues 1294−1430 and/or 1497−1531 within NBD2 has been mapped intracellularly (*41*).

To distinguish between a four and a six TM domain model for MAR3 of MRP, we have used epitope insertion and immunofluorescence to identify intra- and extracellular loops in this segment of the protein. The 10 amino acid HA epitope was inserted within predicted hydrophilic peaks identified by hydropathy analysis in the carboxy-terminal MAR3 of MRP. These mutant proteins were expressed in HeLa cells to test their capacity to confer drug resistance, and the polarity of the inserted HA epitopes with respect to the plasma membrane (intra- vs extracellular) was determined by immunofluorescence in intact or permeabilized cells using a monoclonal antibody directed against the epitope tag.

EXPERIMENTAL PROCEDURES

Materials. Genetycin (G418) was obtained from Gibco BRL Life Technology Inc. (Burlington, Ontario), vincristine (VCR) was obtained from Sigma Chemicals Co. (St. Louis, MO), and etoposide (VP-16), Adriamycin (ADM), and actinomycin-D (ACT) were obtained from the Royal Victoria Hospital, Montreal, Quebec. All restriction enzymes were obtained from New England Biolabs (Mississauga, Ontario) or Pharmacia Biotech Inc (Baie d'Urfe, Quebec). The protein assay reagent was from Bio-Rad Laboratories Ltd (Mississauga, Ontario), and the oligonucleotide-directed in vitro mutagenesis system (version 2.1, RPN 1523) was from Amersham Canada (Oakville, Ontario). The monoclonal anti-hemagglutinin A antibody 16B12 (Babco Labs, Richmond, CA), the monoclonal anti-MRP antibody QCRL-1 (ID Laboratories, London, Ontario), and the goat anti-mouse secondary antibody conjugated to rhodamine (TRITC; Jackson Immuno Research Laboratories; Mississauga, Ontario) were purchased commercially. The HeLa cells were obtained from the American Type Culture Collection (ATCC; Rockville, MD). The full-length human *MRP1* cDNA was a gift of Drs. R. Deeley and S. Cole (Queen's University, Kingston, Ontario).

Site-Directed Mutagenesis. HA epitopes were inserted at discrete locations in MRP as 10 amino acid peptides (YPYDVPDYAS) by site-directed mutagenesis of the cDNA, as described previously (*32*). In addition, the mutagenic oligonucleotides were designed to contain a unique *Nhe*I site to facilitate the insertion of additional tags. The position of each inserted epitope relative to the amino acid sequence of the protein is given in Figure 1, and the oligonucleotides used for mutagenesis are shown in Table 1. Briefly, a full-length cDNA for human *MRP* cloned into the plasmid vector pBluescript (pBl/*MRP*) was digested with *Sma*I, and a 2-kb restriction fragment (pst 2336 to pst 4322) that corresponds to the 3′ half of the *MRP* cDNA was cloned into the *Sma*I site of M13mp18 (M13/*MRP*). To facilitate subsequent cloning procedures, two silent mutations generating novel *Mlu*I (pst 2606; mutagenic oligonucleotide 3′ GACGCATGGATGCGCAGGTGTCTCGTCCTCG 5′) and *BsiW*I (pst 3196; mutagenic oligonucleotide 3′ CTCGAAGAAACTCGCATGCGGGTCACCCTTGGAC 5′) restriction sites were introduced in the *MRP* cDNA. For this, mutagenic oligonucleotides were annealed to a single-stranded M13/*MRP* DNA template, and mutagenesis was carried out using a commercially available in vitro kit. The 2-kb *Sma*I fragment containing novel *Mlu*I and *BsiW*I sites was reinserted into pBl/*MRP* prior to cloning the full-length modified *MRP* cDNA (as a *Sac*I to *Kpn*I fragment) into the mammalian expression vector pCB6 (*44*). Insertional mutagenesis in the carboxy-terminal half of *MRP* (constructs 1, 2a, 3, 4, 5a) was carried out by in vitro mutagenesis using a single-stranded M13/*MRP* DNA template and the oligos listed in Table 1. The integrity of the mutagenized *MRP* cDNA inserts was verified by nucleotide sequencing (*45*), and the modified *MRP* cDNA inserts were subcloned either as *Mlu*I/*BsiW*I (constructs 1, 2a) or *BsiW*I/*Eco*RI (constructs 3, 4, 5a) fragments into pCB6/*MRP*. In the case of mutants 2b, 5b, and 6, the HA epitope was introduced by cloning a short double-stranded segment composed of two complementary oligonucleotides into pre-existing restriction sites, as previously described (*33*). HA epitopes were inserted in this way at nucleotide pst 3885 (*Eco*RI site), using oligos with cohesive ends compatible with the cloning site. A similar cloning strategy was used to insert a second HA epitope into constructs 2b and 5b, using the unique *Nhe*I site present in the first inserted HA epitope.

Cell Culture. Drug-sensitive human HeLa cells (ATCC) were grown in Dulbecco's modified Eagle's medium (DMEM high glucose) supplemented with 10% fetal calf serum, 2 mM glutamine, penicillin (50 units/mL), and streptomycin (50 μg/mL). pCB6/*MRP* constructs were transfected into

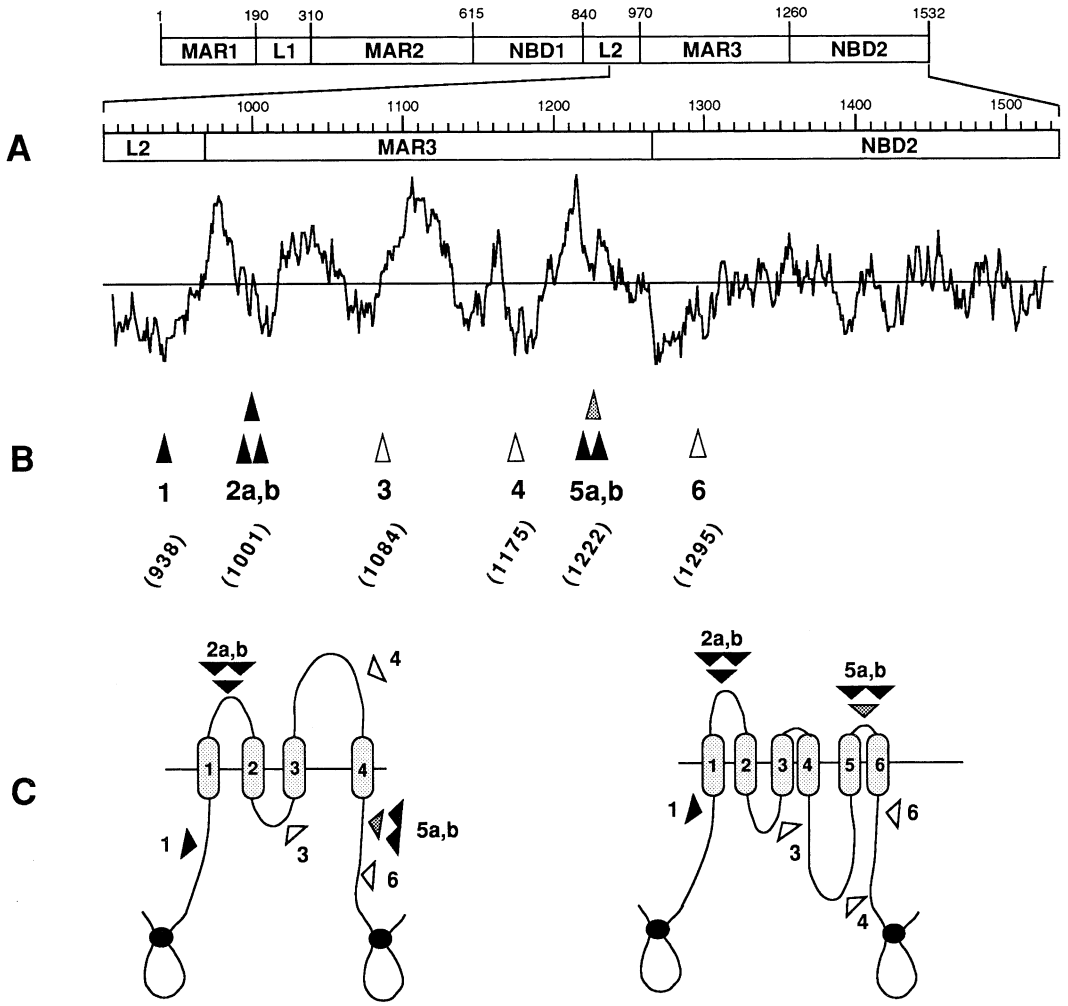

FIGURE 1: Epitope insertion in the membrane-associated region of the carboxy-terminal half of MRP. (A) Hydropathy analysis of MRP (amino acids 970−1532) calculated by the algorithm of Kyte and Doolittle (*49*) and schematic representation of key secondary structural features of the carboxy-terminal half of MRP, including the hydrophobic membrane-associated regions (MAR1, MAR2, and MAR3), nucleotide binding sites (NBD1 and NBD2), and the linker segments (L1, L2) joining the NBDs to the MAR segments. The approximate amino acid positions are indicated. (B) Insertion sites for the YPYDVPDYAS hemagglutinin A (HA) epitopes. The modified proteins are identified with the numbers 1−6 with the amino acid residue preceding the epitope insertion site identified in parentheses. Solid triangles indicate insertion sites that produced functional proteins and in which the tag could be mapped by immunofluorescence. Dotted triangles indicate insertion sites that produced functional proteins but in which the tag could not be mapped by immunofluorescence, and open triangles identify insertions that inactivated the protein. Single triangles represent single epitope tags and double triangles represent two epitope tags side by side. (C) Two alternate topological models for the carboxy-terminal half of MRP, including a four-TM model based on hydropathy analyses and a six TM domain model based on multiple sequence alignment of several ABC transporters (*8*, *37*, *39*).

HeLa cells by calcium phosphate coprecipitation, as we have described previously (*32*). After 2 days, cells were subcultured at a 1:5 dilution, and stable transfectants were selected in medium containing G418 (600 μg/mL). Mass populations of G418^R transfectants were harvested after 9 days and subcultured in medium containing the etoposide VP-16 (final concentration 250 ng/mL) to select mass populations of drug-resistant cell clones overexpressing the tagged MRP proteins. VP-16^R populations were harvested 1−2 weeks later, expanded in culture, and frozen at −80 °C in 90% serum and 10% DMSO.

Membrane Preparation and Western Blotting. Crude membrane fractions from transfected HeLa cells were isolated as described previously (*46*). Briefly, cells were grown to 70% confluency and harvested in cold phosphate-buffered saline (PBS) containing sodium citrate. The cell pellet was homogenized (Dounce homogenizer, 25 strokes) in buffer containing 1 mM $MgCl_2$ and 10 mM Tris, pH 7.0 supplemented with protease inhibitors leupeptin (2 μg/mL), aprotinin (2 μg/mL), and pepstatin (1 μg/mL). Unbroken cells and nuclei were removed by centrifugation (400 g/10 min), and a crude membrane fraction was prepared by centrifugation of the supernatant fraction at 100000*g* for 60 min. The protein concentration in the crude membrane fraction was determined by the method of Bradford, using a commercially available reagent (Bio-Rad). For immunodetection of recombinant MRP, 25 μg of protein was resolved on a SDS-containing 7.5% polyacrylamide gel (SDS−PAGE) and transferred by electroblotting to nitrocellulose membranes. The immunoblots were incubated with the monoclonal anti-HA antibody 16B12 at a 1:3000 dilution or the MRP-specific monoclonal antibody QCRL-1 at a 1:100 dilution, and specific immune complexes were revealed using a horseradish peroxidase conjugated sheep anti-mouse antibody (1:10000 or 1:5000, respectively) (Amersham).

Cytotoxicity Assay. Drug cytotoxicity assays were performed using sulforhodamine B to stain cellular proteins, as described previously (*47*). For this, 6×10^3 cells from VP-

Table 1: Oligonucleotides Used for Epitope Insertion by Site-Directed Mutagenesis

1	(2800) CTG	CAG	AAA	GCT	**E**938[1] GAG	(HA epitope)[2]	**A**939 GCC	AAG	AAG	GAG	GAG	(2829)	
2a	(2988) C AGC	CTC	TGG	ACT	**D**1001 GAT	(HA epitope)[2]	**D**1002 GAC	CCC	ATC	GTC	AAC	(3018)	
2b					**D**1001	(HA epitope)[2] x 2	**D**1002						
3	(3238) CTG	GAC	ACA	GTG	**D**1084 GAC	(HA epitope)[2]	**M**1086 ATG	ATC	CCG	GAG	GTC	A (3271)	
4	(3511) CAG	GAG	CGC	TTC	**I**1175 ATC	(HA epitope)[2]	**H**1176 CAC	CAG	AGT	GAC	CT (3539)		
5a	(3653) CG	GTG	ATC	TCC	**R**1222 AGG	(HA epitope)[2]	**H**1223 CAC	AGC	CTC	AGT	GC (3680)		
5b					**R**1222	(HA epitope)[2] x 2	**H**1223						
6					**F**1295	(HA epitope)[3]	**R**1296						

(HA epitope)[2]: **Y P Y D V P D Y A S**

(HA epitope)[3]: **Y P Y D V P D Y A S E F**

[1] Amino acid residue immediately preceding the site of insertion of the influenza virus hemagglutinin (HA) epitope which sequence is shown [2,3].

16^R mass populations expressing independently tagged MRP proteins and drug-sensitive HeLa control cells were seeded in 96-well titer plates with DMEM medium containing increasing concentrations of ADM, ACT, VCR, or VP-16. The cells were incubated at 37 °C for 96 h and fixed in 17% trichloroacetic acid in PBS, and cellular protein was stained for 10 min at room temperature with 0.4% sulforhodamine B in a 1% acetic acid solution. The plates were washed with water and dried, and the stain was dissolved in 0.2 mL of 10 mM Tris (pH 9). Quantification of sulforhodamine B was done using an automated ELISA plate reader (Bio-Rad Model 450) at a wavelength of 490 nm. The relative plating efficiency of each clone was determined by dividing the absorbance observed at a given drug concentration by the absorbance detected in the same clone in the absence of drug.

Immunofluorescence. Localization of the epitope was performed by immunofluorescence on 3×10^4 cells from $VP\text{-}16^R$ mass populations of individually tagged *MRP* transfectants that had been grown on glass coverslips for 2 days. Drug-sensitive HeLa cells were used as a negative control. Nonpermeabilized HeLa cells were first incubated with the monoclonal antibody 16B12 (1:250) in PBS containing 5% goat serum and 1% bovine serum albumin (BSA) for 1 h at 4 °C. The cells were then fixed in 4% paraformaldehyde in PBS, and they were permeabilized and blocked with PBS containing 0.05% Nonidet-P40, 5% goat serum, and 1% BSA at room temperature for 15 min. A secondary antibody (rhodamine-conjugated goat anti-mouse IgG) was applied in the same buffer (1:200 dilution). In experiments with permeabilized cells, the cells were fixed and permeabilized as described above and blocked with PBS containing 0.05% Nonidet-P40, 5% goat serum, and 1% BSA. The cells were then incubated with the primary antibody (1:1000 dilution) for 1 h at room temperature prior to exposure to the secondary antibody (1:200 dilution). Immunofluorescence microscopy was performed using standard epifluorescence optics (Nikon).

RESULTS

Construction and Expression of Epitope-Tagged Mutant MRPs. Hydropathy analysis suggests that MRP is composed of two hydrophilic ATP-binding domains (amino acids ~615−840, NBD1; ~1260−1532, NBD2), two membrane-associated regions in the amino-terminal half of the protein (amino acids ~1−190, MAR1; ~310−615, MAR2), and one membrane-associated region in the C-terminal half (residues ~970−1260, MAR3) (Figure 1A). Previously, we used epitope insertion and immunofluorescence to investigate the membrane topology of the two hydrophobic regions MAR1 and MAR2 encoded by the amino-terminal half of MRP (*38*). Here we have used a similar experimental strategy to probe the topology of the carboxy-terminal half of MRP (MAR3, residues 938−1295). For this, the antigenic epitope tag YPYDVPDYAS (hemagglutinin, HA) was independently inserted within the most hydrophilic peaks of MAR3 (Figure 1A) at amino acid positions 938 (construct 1), 1001 (construct 2a), 1084 (construct 3), 1175 (construct 4), 1222 (construct 5a), and 1295 (construct 6) (Figure 1B). Since the single epitopes inserted at positions 1001 and 1222 were found to be poorly accessible to the antiepitope antibody in immunofluorescence experiments (see below), two consecutive copies of the HA epitope were inserted at these positions (constructs 2b and 5b, respectively). This strategy has been previously used to increase accessibility of protease cleavage sites in extracellular loops of the lactose permease of *Escherichia coli* (*48*) and also to map the extracellular loops of P-gp (*33*). The wild-type *MRP* and mutant HA-tagged *MRP* cDNAs were cloned into the mammalian expression vector pCB6 and transfected into HeLa cells. Stable transfectants were selected in G418, and mass populations of $G418^R$ colonies were further selected in VP-16 (250 ng/mL). Drug-resistant colonies emerged within 1−2 weeks of selection in populations of $G418^R$ cells transfected with wild-type *MRP* or with *MRP* constructs 1, 2a, 2b, 5a, and

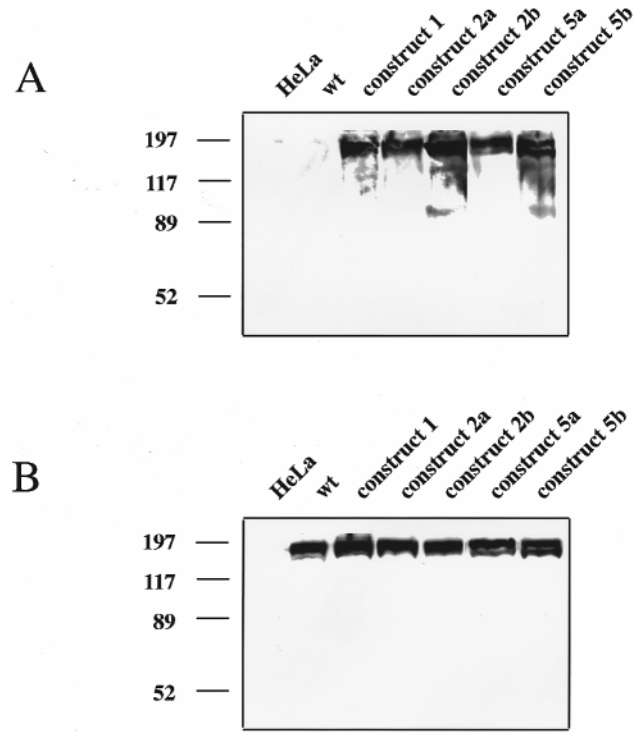

FIGURE 2: Expression of the epitope-tagged MRP constructs 1, 2a, 2b, 5a, and 5b in HeLa cells. HeLa cells were transfected with wild-type (WT) or mutant *MRP* cDNAs containing HA epitopes and selected in drug-containing medium. Crude membrane fractions were isolated from mass populations of VP-16^R transfected cells. Twenty-five micrograms of protein was loaded in each lane, resolved by 7.5% SDS−polyacrylamide gel electrophoresis and analyzed by immunoblotting with the anti-HA epitope antibody 16B12 (panel A) and the monoclonal anti-MRP antibody QCRL-1 (panel B). The positions of the molecular mass markers (in kDa) are shown on the left side of the figure.

5b. However, selection in VP-16 of cells transfected with the pCB6 vector alone or with constructs 3, 4, and 6 yielded no drug-resistant colonies, even after 4 weeks of selection. These results indicated that an HA epitope inserted at position 938 or two HA epitopes at positions 1001 and 1222 were compatible with the MRP protein function. On the other hand, insertion of HA epitopes at positions 1084, 1175, and 1295 caused an apparent loss of MRP function.

Expression of the modified MRP proteins in HeLa cells was analyzed by Western blotting (Figure 2A,B). Crude membrane fractions from control, nontransfected HeLa cells and from VP-16^R mass populations expressing either wild-type *MRP* or constructs 1, 2a, 2b, 5a, and 5b were separated on a 7.5% SDS−PAGE, transferred to a blotting membrane, and analyzed using the anti-HA epitope antibody 16B12 (Figure 2A). Specific immunoreactive bands of ~180 kDa were observed in membrane fractions from all VP-16^R *MRP* transfectants, and these bands were absent in membranes from nontransfected control HeLa cells or membranes from VP-16^R cells transfected with the wild-type *MRP* cDNA (Figure 2A). Immunoblotting of the same membrane preparations was also carried out using the anti-MRP antibody QCRL-1 directed against an epitope located in the linker region connecting NBD1 to the C-terminal half of the protein (*42*, *43*) (Figure 2B). As expected, a similar immunoreactive band at ~180 kDa was detected by this antibody in membrane fractions from all VP-16^R *MRP* transfectants, and this band was absent in membranes from control HeLa cells (Figure 2B), indicating that the biologically active HA-tagged MRP proteins encoded by constructs 1, 2a, 2b, 5a, and 5b were expressed in the membrane fraction of these transfectants. These results indicated that HA-epitope insertion in these constructs did not drastically affect MRP protein targeting or function.

Drug Resistance Profiles of Mutant Proteins 1, 2a, 2b, 5a, and 5b. To determine whether insertion of HA epitopes might have more subtle effects on MRP function, the drug survival characteristics of VP-16^R mass populations expressing constructs 1, 2a, 2b, 5a, and 5b were established for known MRP substrates. The cells were plated in increasing concentrations of Adriamycin (ADM), actinomycin-D (ACT), etoposide (VP-16), and vincristine (VCR) (Figure 3), and the drug concentration required to reduce the plating efficiency of each mass population by 50% (IC50) was calculated. All mass populations of cells expressing these epitope-tagged proteins displayed similar resistance levels to ADM (fold resistance: 5−9×), ACT (fold resistance; 4−6×), VCR (fold resistance: 8−15×), and VP-16 (fold resistance: 9−12×), and these levels were comparable to resistance levels measured in transfectants expressing wild-type MRP. These results indicated that epitope insertions at positions 938, 1001, and 1222 were without noticeable functional consequences on MRP protein function.

Localization of the Epitope Tags. To determine the polarity of the epitopes with respect to the plasma membrane, immunofluorescence was performed using the anti-HA monoclonal antibody 16B12 on VP-16^R transfectants expressing individual HA-tagged MRP proteins. Immunofluorescence was carried out on both intact cells and cells permeabilized with NP-40 to detect extracellular and intracellular tags, respectively (Figure 4). No significant cell-associated fluorescence could be detected with the antibody in intact or permeabilized control HeLa cells or in cells expressing the wild-type MRP protein (Figure 4A,B). On the other hand, cells that expressed mutant proteins 2b (amino acid position 1001) and 5b (amino acid position 1222) gave a strong fluorescent signal in both intact and permeabilized cells (Figure 4E−H). This unambiguously demonstrated the extracellular location of the HA epitope in these MRP variants. In contrast, mass populations of cells expressing mutant protein 1 (position 938) showed bright fluorescence only in permeabilized cells (Figure 4D), but not in intact cells (Figure 4C), suggesting an intracellular location of the HA epitope in this MRP variant. Transfectants expressing construct 1 also showed perinuclear staining in permeabilized cells in addition to the plasma membrane staining (Figure 4D).

Transfectants expressing mutants 2a and 5a, which contain single HA epitopes inserted at positions 1001 or 1222, either were weakly immunoreactive (construct 2a, data not shown) or did not react at all (construct 5a, data not shown) with the anti-HA antibody. Addition of a second consecutive HA epitope at positions 1001 (mutant 2b) and 1222 (mutant 5b) allowed the unambiguous localization of these segments of MRP to the extracellular face of the membrane, as noted by the reactivity of the antibody in intact cells (Figure 4E,G). However, the fluorescent signal observed in 5b transfectants was still modest compared to that seen with other extracellular epitopes, in agreement with the proposition that the antibody has limited access to this epitope. Nevertheless,

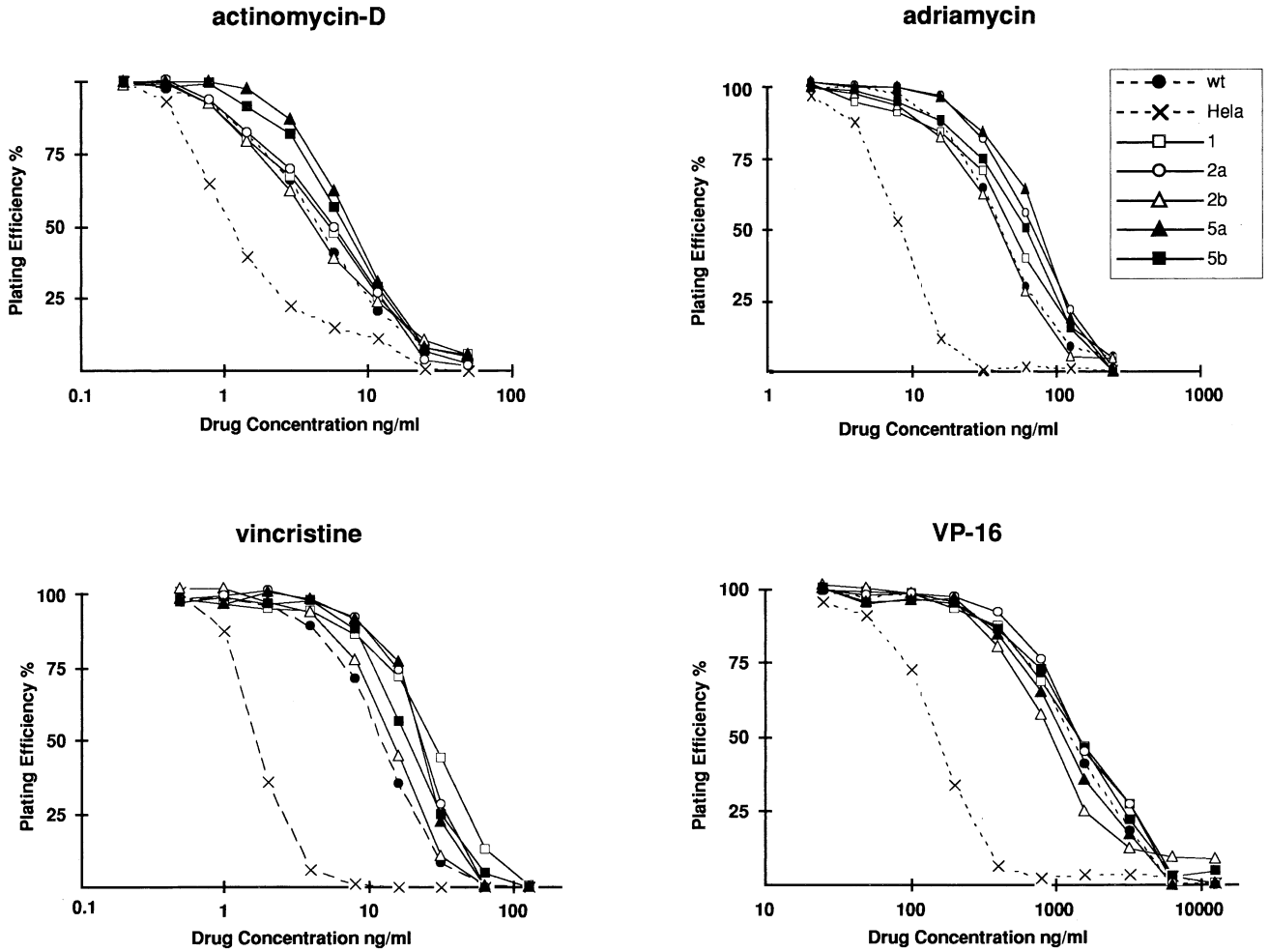

FIGURE 3: Drug survival characteristics of control HeLa cells and drug-resistant MRP transfectants expressing wild-type (WT) or mutant proteins 1, 2a, 2b, 5a, and 5b. Control drug sensitive HeLa cells (X, stippled line) and mass populations corresponding to either wild-type *MRP* (●, dashed line) or *MRP* constructs 1 (□), 2a (○), 2b (△), 5a (▲), and 5b (■) were plated in increasing concentrations of ADM, ACT, VCR, or VP-16 and incubated for 96 h. Drug cytotoxicity was measured using a sulforhodamine B staining procedure. The relative plating efficiency of each cell population was calculated by dividing the absorbance measured at a given drug concentration by the value obtained for the same clone in the absence of drug, and it was expressed as a percentage (%). Each point represents the average of at least two independent experiments performed in duplicate.

these experiments provided topological data for three insertion sites in the MAR3 segment of MRP.

DISCUSSION

Hydropathy analysis of the primary amino acid sequence of the MRP subgroup of ABC transporters identifies a unique, very hydrophobic segment at their amino termini which is absent in other ABC transporters such as P-gp and CFTR (*35*, *36*). This novel segment and its associated linker are approximately 300 residues in length and probably account for the size difference between P-gp (*35*, *36*) and the MRP-related proteins cMOAT (*rMrp2*; *16*, *17*), YCF1 (yeast cadmium resistance factor, *21*), YORI (yeast oligomycin resistance, *22*), BAT1 (bile acid transporter in yeast, *23*), SUR1 and SUR2 (rat sulfonylurea receptors, *26*, *27*), EBCR (cAMP-activated epithelial basolateral chloride conductance regulator, *28*), and P-gpA (arsenicals resistance in *Leishmania*, *24*, *25*). Apart from this unique hydrophobic MAR1 segment, the rest of the hydropathy profile of MRP, including the MAR2 and MAR3 regions, resembles that of other ABC transporters, including P-gp and CFTR (*35*, *36*). Direct topological analysis by epitope insertion and using single cysteine mutants showed that these regions of P-gp and CFTR code for six TM domains each (*31*−*34*), indirectly supporting a similar six-TM model for the MAR2 and MAR3 regions of MRP. On the other hand, topological models for MAR3 consisting of four TM segments cannot be excluded (*8*, *37*).

We have previously used epitope insertion and immunofluorescence to study the membrane topology of P-gp (*32*, *33*) and that of the MAR1 and MAR2 region of MRP (*38*). This method is based on the direct analysis of epitope-tagged but functional proteins capable of conferring drug resistance in mammalian cells, thus providing a normal physiological background with proper post-translational modifications, such as phosphorylation and glycosylation. Epitope tags from influenza hemagglutinin A protein (HA) were inserted in the MAR3 region of MRP at positions showing the highest hydrophilicity values (Figure 1A) and which are therefore most likely located in extracellular or intracellular loops linking individual TM segments. We also introduced an HA epitope within the linker region connecting NBD1 to the MAR3 and another one in the NBD2. The modified proteins were then expressed in mammalian cells so that any

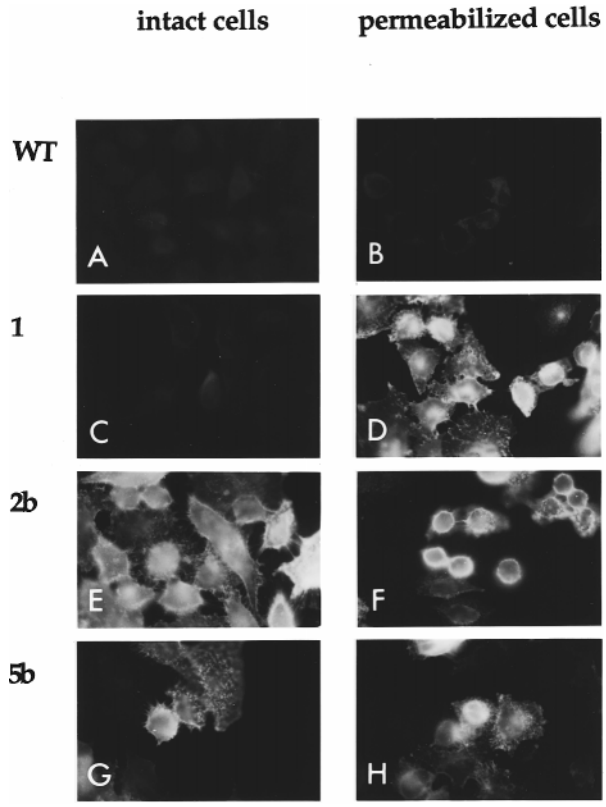

FIGURE 4: Detection of epitope-tagged MRP proteins by immunofluorescence. HeLa cell transfectants stably expressing wild-type MRP (WT) mutant MRP 1, 2b, or 5b were exposed to the mouse monoclonal anti-HA epitope antibody 16B12 without pretreatment (intact cells, left column) or with pretreatment with 0.05% NP-40 (permeabilized cells, right column). Cells were then incubated with a secondary goat anti-mouse antibody conjugated to rhodamine (TRITC), and the cells were photographed using a fluorescence microscope. The HA epitopes in constructs 2b (E, F) and 5b (G, H) were detected in nonpermeabilized and permeabilized cells, while the HA epitope in construct 1 (C, D) was only detectable in permeabilized cells. For photography, all exposure times were identical.

deleterious effect of epitope insertion on MRP function could be monitored, and the accessibility of the epitope to the anti-HA tag antibody 16B12 was determined in intact and permeabilized cells to establish membrane polarity of the tag. Using this approach, we have localized double HA epitopes inserted at positions 1001 and 1222 to the extracellular side of the membrane and an HA epitope inserted at position 938 to the intracellular side of the membrane (Figure 4). While our experimental method allowed unambiguous determination of the extracellular epitopes (constructs 2b and 5b), the assignment of the intracellular HA epitope of construct 1 was tentative, since cells expressing this construct (epitope at position 938) showed intracellular staining in addition to plasma membrane staining. This indicates that only a portion of the MRP variant was expressed at the plasma membrane, while a portion was retained in the endoplasmic recticulum or the Golgi apparatus. This suggests that epitope insertion at this position may partly impede or slow maturation or processing of the protein through the cellular membranous compartments. However, it is clear that at least part of construct 1 is correctly folded and reaches the plasma membrane, since construct 1 could confer drug resistance levels similar to those seen for the wild-type protein. Furthermore, the intracellular localization of the HA tag at position 938 predicted from our analysis is in agreement with the previous localization of the neighboring 918−924 segment (QCRL-1 antibody epitope) to the intracellular side of the plasma membrane (*43*).

Insertion of single epitopes at amino acid positions 1084, 1175, and 1295 abrogated MRP function, preventing mapping of these sites by our approach. Epitope tags inserted at these sites may interfere with protein folding or targeting or may affect structural and functional domains that are essential for the drug transport activity of the protein. Single epitope insertions at positions 1001 and 1222 were compatible with MRP function, but these epitopes could not be detected by immunofluorescence very easily. Insertion of a second HA epitope at these positions enabled localization by immunofluorescence. The extracellular loops containing positions 1001 and 1222 may be fairly short and in close proximity to the plasma membrane and therefore may be difficult to access for the antibody. Insertion of a second epitope tag to enlarge the loop appears necessary in this case for immunoreactivity with the anti-HA antibody. The Western blots from membrane fractions of most transfectants showed a second additional MRP species of faster electrophoretic mobility (∼160 kDa) which was immunoreactive with both the anti-HA and the anti-MRP antibodies. The nature of this protein isoform is unclear, but it may represent a less mature, partially glycosylated form of MRP. We have previously noted in similar experimental settings such isoforms of P-gp (*32*, *33*) and MRP (*38*) with altered electrophoretic mobility. The presence or relative abundance of such isoforms is variable and does not correlate with changes in biological activity of these two proteins.

Although hydropathy profiling (*36*) suggests a six-TM structure for MAR3, the direct topological data currently available for this region do not allow one to formally distinguish between a four- and six-TM structure (*37*, *40*). The two NBDs have been clearly localized intracellularly, on the basis of access to the ATP substrate, mapping of a trypsin cleavage site, and epitope mapping of the anti-MRP antibody QCRL-1 directed against the 918−924 peptide epitope to the L2 region linking NBD1 to MAR3 (*40*, *43*). Our assignment of an epitope tag at position 938 to the intracellular side of the membrane (Figure 5) is in agreement with these results. The intracellular location of NBD2, on the other hand, has been verified using antibodies directed against recombinant proteins corresponding to positions 1294−1430 fused to 1497−1531 (*41*). Anchoring a topological model for the carboxy-terminal half of MRP to the two intracellular NBDs suggests an even number of four or six TM domains for MAR3. Our localization of an epitope inserted at amino acid position 1001 to the extracellular side of the membrane is compatible with either model (Figure 1C, constructs 2a and 2b). Likewise, the demonstration that Asn^{1006} is indeed glycosylated in vivo (*37*) also supports an extracellular localization of this segment but does not distinguish between the four- and six-TM models. However, the positioning of an HA epitope inserted at position 1222 to the extracellular side of the membrane (Figure 1C, constructs 5a and 5b) is incompatible with a four-TM model for MAR3 which would place this epitope on the intracellular side. Consequently, our studies by epitope

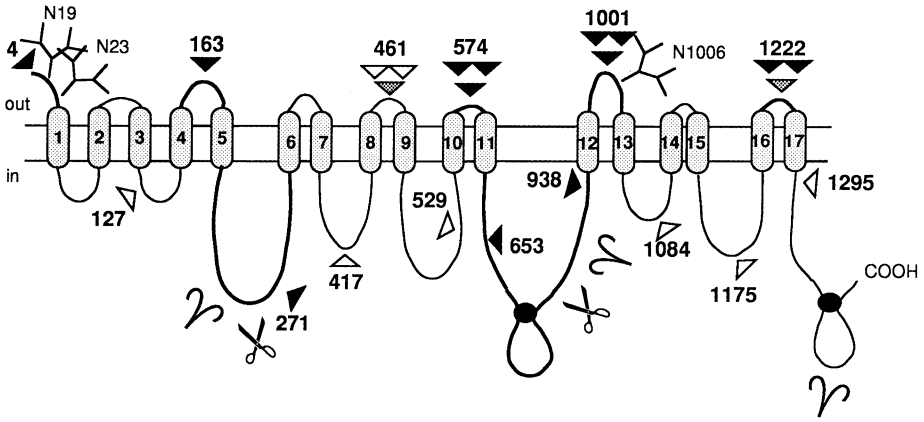

FIGURE 5: Proposed membrane topology of MRP as determined by epitope insertion. Immunofluorescence with HA epitopes confirmed the extracellular localization of epitopes inserted in the carboxy-terminal half of MRP at positions 1001 and 1222, and the cytoplasmic localization of an epitope inserted within L2 at amino acid position 938. Using the same method to determine the topology of the amino-terminal half of MRP, we had previously determined the extracellular location of epitopes inserted at amino acids 4, 163, and 574 and the intracellular location of epitopes inserted at amino acids 271 (within L1) and 653 (within NBD1) (38). Loops for which an unambiguous intra- or extracellular localization has been established are drawn with a fat pen. Filled arrowheads indicate the position of HA epitope insertions that resulted in functional MRPs, while empty arrowheads indicate the position of HA epitopes which abrogate MRP function. Dotted arrowheads indicate the position of the HA epitope insertions that resulted in functional MRPs but in which the epitope tag could not be localized by immunofluorescence. Single triangles represent a single epitope, whereas double triangles represent two contiguous epitopes. The position of the nucleotide binding site is identified by a filled circle. Protease cleavage sites mapped by Bakos et al. (*40*) and Hipfner et al. (*43*) are indicated by scissors and antibody recognition sites mapped by Flens et al. (*41*), Hipfner et al. (*43*), and Bakos et al. (*40*) by curved v's. Finally, the position of Asn residues known to be modified by N-linked glycosylation (Asn^{19}, Asn^{23}, Asn^{1006}) (*37*) are also shown.

mapping together with studies of glycosylation site mutants (*37*) and hydropathy profiling (*36*) suggest the following six TM domain model for MAR3 (Figure 1C, right panel; Figure 5): the first TM would be located between intracellular position 938 and extracellular position 1001, as shown here by epitope insertion (constructs 1 and 2b, respectively) and elsewhere by glycosylation studies (*37*). The second TM would be positioned within the hydrophobic segment encompassing amino acids ~1015−1050, while the third hydrophobic region between positions ~1080 and 1130 is wide enough to encompass two TM domains, as is the case for the homologous segments of P-gp and CFTR (*31*−*34*). The fifth TM would be positioned between amino acid positions ~1195 and 1220 with an additional and final TM domain located between the mapped extracellular epitope at position 1222 (construct 5b) and the intracellular ATP-binding domain (encompassing amino acids ~1225−1250).

The combined topological data from epitope mapping (*38*; this study) and other studies (*36*, *37*, *40*−*43*) is summarized in Figure 5. It suggests that MRP contains 11 TM domains in the first half of the protein (MAR1, MAR2) and six TM domains in the second half (MAR3), for a total of 17 TM domains (Figure 5). This is in agreement with the model originally proposed by Tusnády et al. (*36*). We (*38*) and others (*37*) have previously mapped the amino terminus of MRP extracellularly and the loop containing amino acid 163 to the extracellular side as well (*38*), while an epitope inserted at position 271 (L1 region) is on the intracellular side of the membrane (*38*). An intracellular localization for L1 is also supported by epitope-mapping studies using an antibody raised against a protein overlapping pst 192−360 which is accessible only in permeabilized cells (*41*) and by the identification of a protease hypersensitive site within this region (*40*, *43*) (Figure 5). These data combined with hydropathy analysis support a five-TM model for MAR1. The six-TM model for MAR2 is derived from computer-based sequence alignments and hydropathy profiling (*36*, *37*). However, a double epitope within MAR2 at amino acid position 574 was mapped on the extracellular side of the membrane (*38*) in agreement with such a model. The cytoplasmic location of the NBD1 and the L2 region, on the other hand, has been verified by mapping the epitope of anti-MRP antibody QCRL-1 (residues 918−924) intracellularly (*42*, *43*), by the presence of a protease hypersensitive site in this region (*40*, *43*), and by our epitope mapping of HA tags inserted at positions 653 and 938 (*38*, this study). Finally, results from this study favor a six-TM model for MAR3, based on the extracellular localization of an epitope inserted at amino acid position 1001 and in particular at position 1222. The intracellular location of NBD2 has been established by others using an antibody against a fusion protein near NBD2 (*41*) which reacts only in permeabilized cells.

Overall, we found that HA epitopes inserted in extracellular loops are much better tolerated to preserve function than epitopes inserted in what should be intracellular loops. Indeed, only three out of nine possibly intracellular sites resulted in functional proteins in which the membrane polarity of the inserted epitope could be mapped. We have previously noted in similar studies of P-glycoprotein that epitope insertions in extracellular loops are much more likely to preserve function than those occurring in intracellular loops (*33*). The integrity of the intracellular loops therefore appears critical for proper protein folding and processing or for some other essential aspect of transport, while extracellular loops seem to tolerate more readily the insertion of short peptide sequences.

ACKNOWLEDGMENT

The authors wish to thank Drs. R. Deeley and S. Cole (Queen's University) for the generous gift of full-length

cDNA for *MRP*. This work was supported by research grants to P.G. from the National Cancer Institute of Canada and the Society du Cancer. P.G. is an International Research Scholar of the Howard Hughes Medical Institute and a Career Scientist of the Medical Research Council of Canada.

REFERENCES

1. Shustik, C., Dalton, W., and Gros, P. (1995) *Mol. Aspects Med. 16*, 1−78.
2. Nooter, K., and Sonneveld, P. (1994) *Leuk. Res. 18*, 233−243.
3. Ota, E., Abe, Y., Oshika , Y., Ozeki, Y., Iwasaki, M., Inoue, H., Yamazaki, H., Ueyama, Y., Takagi, K., Ogata, T., Tamaoki, N., and Nakamura, M. (1995) *Br. J. Cancer 72*, 550−554.
4. Ruetz, S., and Gros, P. (1994) *J. Biol. Chem. 269*, 12277−12284.
5. Cole, S. P. C., Sparks, K. E., Fraser, K., Loe, D. W., Grant, C. E., Wilson, G. M., and Deeley, R. G. (1994) *Cancer Res. 54*, 5902−5910.
6. Zaman, G. J. R., Flens, M. J., van Leusden, M. R., de Haas, M., Mülder, H. S., Lankelma, J., Pinedo, H. M., Scheper, R. J, Baas, F., Broxterman, H. J., and Borst, P. (1994) *Proc. Natl. Acad. Sci. U.S.A. 91*, 8822−8826.
7. Loe, D. W., Almquist, K. C., Deeley, R. G., and Cole, S. P. C. (1996) *J. Biol. Chem. 271*, 9675−9682.
8. Cole, S. P. C., Bhardwaj, G., Gerlach, J. H., Mackie, J. E., Grant, C. E., Almquist, K. C., Stewart, A. J., Kurz, E. U., Duncan, A. M. V., and Deeley, R. G. (1992) *Science 258*, 1650−1654.
9. Grant, C. E., Valdimarsson, G., Hipfner, D. R., Almquist, K. C., Cole, S. P. C., and Deeley, R. G. (1994) *Cancer Res. 54*, 357−361.
10. Jedlitschky, G., Leier, I., Buchholz, U., Center, M., and Keppler, D. (1994) *Cancer Res. 54*, 4833−4836.
11. Leier, I., Jedlitschky, G., Buchholz, U., Cole, S. P. C., Deeley, R. G., and Keppler, D. (1994) *J. Biol. Chem. 269*, 27807−27810.
12. Müller, M., Meijer, C., Zaman, G. J. R., Borst, P., Scheper, R. J., Mulder, N. H., de Vries, E. G. E., and Jansen, P. L. M. (1994) *Proc. Natl. Acad. Sci. U.S.A. 91*, 13033−13037.
13. Loe, D. W., Almquist, K. C., Cole, S. P. C., and Deeley, R. G. (1996) *J. Biol. Chem. 271*, 9683−9689.
14. Jedlitschky, G., Leier, I., Buchholz, U., Barnouin, K., Kurz, G., and Keppler, D. (1996) *Cancer Res. 56*, 988−994.
15. Kool, M., de Haas, M., Scheffer, G. L., Scheper, R. J., van Eijk, M. J. T., Juijn, J. A., Baas, F., and Borst, P. (1997) *Cancer Res. 57*, 3537−3547.
16. Paulusma, C. C., Bosma, P. J., Zaman, G. J. R., Bakker, C. T. M., Otter, M., Scheffer, G. L., Scheper, R. J., Borst, P., and Oude Elferink, R. P. J. (1996) *Science 271*, 1126- 1128.
17. Büchler, M., König, J., Brom, M., Kartenbeck, J., Spring, H., Horie, T., and Keppler, D. (1996) *J. Biol. Chem. 271*, 15091−15098.
18. Kartenbeck, J., Leuschner, U., Mayer, R., and Keppler D. (1996) *Hepatology 23*, 1061−1066.
19. Paulusma, C. C., Kool, M., Bosma, P. J., Scheffer, G. L., Borg, F. T., Scheper, R. J., Tytgat, G. N. J., Borst, P., Baas, F., and Oude Elferink, R. P. J. (1997) *Hepatology 25*, 1539−1542.
20. Higgins, C. F. (1992) *Annu. Rev. Cell Biol. 8*, 67−113.
21. Szczypka, M. S., Wemmie, J. A., Moye-Rowley, W. S., and Thiele, D. J. (1994) *J. Biol. Chem. 269*, 22853−22857.
22. Katzmann, D. J., Hallstrom, T. C., Voet, M., Wysock, W., Golin, J., Volckaert, G., and Moye-Rowley, W. S. (1995) *Mol. Cell. Biol. 15*, 6875−6883.
23. Ortiz, D. F., St. Pierre, M. V., Abdulmessih, A., and Arias, I. M. (1997) *J. Biol. Chem. 272*, 15358−15365.
24. Ouellette, M., Fase-Fowler, F., and Borst, P. (1990) *EMBO J. 9*, 1027−1033.
25. Callahan, H. L., and Beverley, S. M. (1991) *J. Biol. Chem. 266*, 18427−18430.
26. Aguilar-Bryan, L., Nichols, C. G., Wechsler, S. W., Clement, J. P., IV, Boyd, A. E., III, González, G., Herrera-Sosa, H., Nguy, K., Bryan, J., and Nelson, D. A. (1995) *Science 268*, 423−426.
27. Inagaki, N., Gonoi, T., Clement, J. P., IV, Wang, C.-Z., Aguilar-Bryan, L., Bryan, J., and Seino, S. (1996) *Neuron 16*, 1011−1017.
28. van Kuijck, M. A., van Aubel, R. A. M. H., Busch, A. E., Lang, F., Russel, F. G. M., Bindels, R. J. M., van Os, C. H., and Deen, P. M. T. (1996) *Proc. Natl. Acad. Sci. U.S.A. 93*, 5401−5406.
29. Gros, P., Croop, J., and Housman, D. (1986) *Cell 47*, 371−380.
30. Riordan, J. R., Rommens, J. M., Kerem, B.-S., Alon, N., Rozmahel, R., Grzelczak, Z., Zielenski, J., Lok, S., Plavsic, N., Chou, J.-L., Drumm, M. L., Iannuzzi, M. C., Collins, F. S., and Tsui, L.-C. (1989) *Science 245*, 1066−1073.
31. Loo, T. W., and Clarke, D. M. (1995) *J. Biol. Chem. 270*, 843−848.
32. Kast, C., Canfield, V., Levenson, R., and Gros, P. (1995) *Biochemistry 34*, 4402−4411.
33. Kast, C., Canfield, V., Levenson, R., and Gros, P. (1996) *J. Biol. Chem. 271*, 9240−9248.
34. Chang, X.-B., Hou, Y.-X., Jensen, T. J., and Riordan, J. R. (1994) *J. Biol. Chem. 269*, 18572−18575.
35. Stride, B. D., Valdimarsson, G., Gerlach, J. H., Wilson, G. M., Cole, S. P. C., and Deeley, R. G. (1996) *Mol. Pharmacol. 49*, 962−971.
36. Tusnády, G. E., Bakos, E., Váradi, A., and Sarkadi, B. (1997) *FEBS Lett. 402*, 1−3.
37. Hipfner, D. R., Almquist, K. C., Leslie, E. M., Gerlach, J. H., Grant, C. E., Deeley, R. G., and Cole, S. P. C. (1997) *J. Biol. Chem. 272*, 23623−23630.
38. Kast, C., and Gros, P. (1997) *J. Biol. Chem. 272*, 26479−26487.
39. Loe, D. W., Deeley, R. G., and Cole, S. P. C. (1996) *Eur. J. Cancer 32A*, 945−957.
40. Bakos, E., Hegedüs, T., Holló, Z., Welker, E., Tusnády, G. E., Zaman. G. J. R., Flens, M. J., Varádi, A., and Sarkadi, B. (1996) *J. Biol. Chem. 271*, 12322−12326.
41. Flens, M. J., Izquierdo, M. A., Scheffer, G. L., Fritz, J. M., Meijer, C. J. L. M., Scheper, R. J., and Zaman, G. J. R. (1994) *Cancer Res. 54*, 4557−4563.
42. Hipfner, D. R., Gauldie, S. D., Deeley, R. G., and Cole, S. P. C. (1994) *Cancer Res. 54*, 5788−5792.
43. Hipfner, D. R., Almquist, K. C., Stride, B. D., Deeley, R. G., and Cole, S. P. C. (1996) *Cancer Res. 56*, 3307−3314.
44. Canfield, V. A., and Levenson, R. (1993) *Biochemistry 32*, 13782−13786.
45. Sanger, F., Nicklen, S., and Coulson, A. R. (1977) *Proc. Natl. Acad. Sci. U.S.A. 74*, 5463−5467.
46. Devault, A., and Gros, P. (1990) *Mol. Cell. Biol. 10*, 1652−1663.
47. Tang-Wai, D. F., Brossi, A., Arnold, L. D., and Gros, P. (1993) *Biochemistry 32*, 6470−6476.
48. Sahin-Toth, M., Dunten, R. L., and Kaback, H. R. (1995) *Biochemistry 34*, 1107−1112.
49. Kyte, J., and Doolittle, R. F. (1982) *J. Mol. Biol. 157*, 105−132.

BI972332V